Relativistic MHD simulations of stellar core collapse and magnetars

José A. Font

VNIVERSITAT DE VALÈNCIA

Collaborators:

Pablo Cerdá-Durán, Michael Gabler & Ewald Müller (MPA)
Nikolaos Stergioulas (Aristotle University Thessaloniki)

Outline of the talk

Introduction: MHD in relativistic astrophysics

Mathematical & Numerical framework

- Ideal GRMHD equations
- Einstein equations (CFC)
- Numerical code

Simulations

- Magneto-rotational core collapse
- Alfvén/shear oscillations in magnetars

Cerdá-Durán, Font & Dimmelmeier, A&A, **474**, 161 (2007)
Cerdá-Durán, Font, Antón & Müller, A&A, **492**, 937 (2008)
Cerdá-Durán, Stergioulas & Font, MNRAS, **397**, 1607 (2009)
Gabler, Cerdá-Durán, Font, Stergioulas & Müller, in prep. (2010)

MHD in relativistic astrophysics

Natural domain of general relativistic hydrodynamics (GRHD) and MHD (GRMHD) is the field of relativistic astrophysics. Play a major role in the description of gravitational collapse leading to the formation of compact objects (neutron stars and black holes).

Most of the numerical applications of general relativistic MHD deal with the topics of black hole accretion and jet formation.

Koide et al (2002)

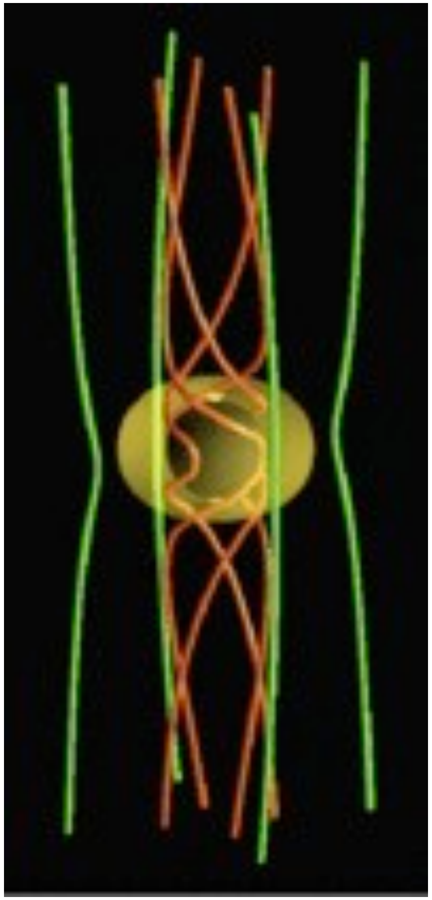

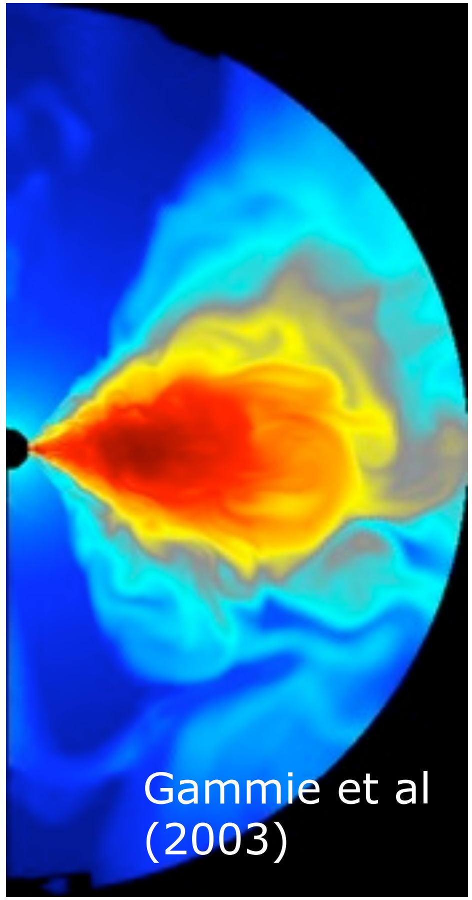

General Relativistic Magneto-Hydrodynamics (1)

GRMHD: Dynamics of relativistic, electrically conducting fluids in the presence of magnetic fields.

Ideal GRMHD: Absence of viscosity effects and heat conduction in the limit of infinite conductivity (perfect conductor fluid).

The stress-energy tensor includes contribution from the perfect fluid and from the magnetic field b^μ measured by observer comoving with the fluid.

$$T^{\mu\nu} = T^{\mu\nu}_{\rm PF} + T^{\mu\nu}_{\rm EM} \quad \longrightarrow \quad \boxed{T^{\mu\nu} = \rho h^* u^\mu u^\nu + p^* g^{\mu\nu} - b^\mu b^\nu}$$

$$T^{\mu\nu}_{\rm PF} = \rho h u^\mu u^\nu + p g^{\mu\nu}$$

$$T^{\mu\nu}_{\rm EM} = F^{\mu\lambda}F^\nu_\lambda - \frac{1}{4}g^{\mu\nu}F^{\lambda\delta}F_{\lambda\delta} = \left(u^\mu u^\nu + \frac{1}{2}g^{\mu\nu}\right)b^2 - b^\mu b^\nu$$

with the definitions:

$$b^2 = b^\nu b_\nu$$

$$p^* = p + \frac{b^2}{2}$$

$$h^* = h + \frac{b^2}{\rho}$$

Ideal MHD condition: electric four-current must be finite.

$$F^{\mu\nu} = -\eta^{\mu\nu\lambda\delta}u_\lambda b_\delta$$

$$F^{\mu\nu}u_\nu = 0$$

$$J^\mu = \rho_{\rm q} u^\mu + \sigma F^{\mu\nu}u_\nu \qquad \sigma \rightarrow \infty$$

General Relativistic Magneto-Hydrodynamics (2)

Conservation of mass: $\nabla_\mu(\rho u^\mu) = 0$

Conservation of energy and momentum: $\nabla_\mu T^{\mu\nu} = 0$

Maxwell's equations: $\nabla_\mu {}^*F^{\mu\nu} = 0$ $\quad {}^*F^{\mu\nu} = \frac{1}{W}(u^\mu B^\nu - u^\nu B^\mu)$

- Divergence-free constraint: $\vec{\nabla} \cdot \vec{B} = 0$
- Induction equation: $\frac{1}{\sqrt{\gamma}}\frac{\partial}{\partial t}\left(\sqrt{\gamma}\vec{B}\right) = \vec{\nabla} \times \left[\left(\alpha\vec{v} - \vec{\beta}\right) \times \vec{B}\right]$

Adding all up: first-order, flux-conservative, hyperbolic system + constraint

$$\frac{1}{\sqrt{-g}}\left(\frac{\partial\sqrt{\gamma}\mathbf{U}}{\partial t} + \frac{\partial\sqrt{-g}\mathbf{F}^i}{\partial x^i}\right) = \mathbf{S} \qquad \frac{\partial(\sqrt{\gamma}B^i)}{\partial x^i} = 0$$

Antón et al. (2006)

$$D = \rho W \qquad S_j = \rho h^* W^2 v_j - \alpha b_j b^0 \qquad \tau = \rho h^* W^2 - p^* - \alpha^2 (b^0)^2 - D$$

$$\mathbf{U} = \begin{bmatrix} D \\ S_j \\ \tau \\ B^k \end{bmatrix} \quad \mathbf{F}^i = \begin{bmatrix} D\tilde{v}^i \\ S_j\tilde{v}^i + p^*\delta^i_j - b_j B^i/W \\ \tau\tilde{v}^i + p^* v^i - \alpha b^0 B^i/W \\ \tilde{v}^i B^k - \tilde{v}^k B^i \end{bmatrix} \quad \mathbf{S} = \begin{bmatrix} 0 \\ T^{\mu\nu}\left(\frac{\partial g_{\nu j}}{\partial x^\mu} - \Gamma^\delta_{\nu\mu} g_{\delta j}\right) \\ \alpha\left(T^{\mu 0}\frac{\partial \ln\alpha}{\partial x^\mu} - T^{\mu\nu}\Gamma^0_{\nu\mu}\right) \\ 0^k \end{bmatrix}$$

In the "test-fluid" approximation (fluid's self-gravity neglected), the dynamics of the matter fields is fully described by the previous conservation laws and the EOS.

When such approximation does not hold, the previous equations must be solved in conjunction with Einstein's equations for the gravitational field which describe the evolution of a dynamical spacetime:

$$R_{\mu\nu} - \frac{1}{2} g_{\mu\nu} R = 8\pi T_{\mu\nu}$$

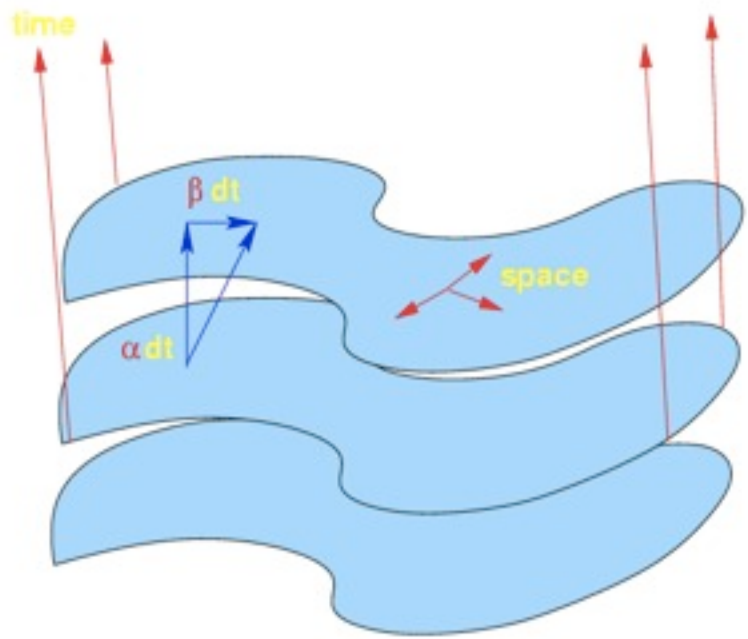

The most widely used approach to solve Einstein's equations in Numerical Relativity is the so-called Cauchy or 3+1 formulation (IVP).

$$ds^2 = -(\alpha^2 - \beta_i \beta^i) dt^2 + 2\beta_i dx^i dt + \gamma_{ij} dx^i dx^j$$

$$\begin{aligned}
\partial_t \gamma_{ij} &= -2\alpha K_{ij} + \nabla_i \beta_j + \nabla_j \beta_i \\
\partial_t K_{ij} &= -\nabla_i \nabla_j \alpha + \alpha \left(R_{ij} + K\, K_{ij} - 2 K_{im} K^m_j \right) + \beta^m \nabla_m K_{ij} \\
&\quad + K_{im} \nabla_j \beta^m + K_{mj} \nabla_i \beta^m - 8\pi\alpha \left(T_{ij} - \frac{1}{2}\gamma_{ij} T^m_m + \frac{1}{2}\rho\gamma_{ij} \right)
\end{aligned}$$

Einstein equations (CFC)

In the CFC approximation (Isenberg 1985; Wilson & Mathews 1996) the ADM 3+1 equations

$$\begin{aligned}
\partial_t \gamma_{ij} &= -2\alpha K_{ij} + \nabla_i \beta_j + \nabla_j \beta_i \\
\partial_t K_{ij} &= -\nabla_i \nabla_j \alpha + \alpha \left(R_{ij} + K\, K_{ij} - 2K_{im} K_j^m \right) + \beta^m \nabla_m K_{ij} \\
&\quad + K_{im} \nabla_j \beta^m + K_{mj} \nabla_i \beta^m - 8\pi\alpha \left(T_{ij} - \frac{1}{2}\gamma_{ij} T_m^m + \frac{1}{2}\rho\gamma_{ij} \right)
\end{aligned}$$

$$\begin{aligned}
R + K^2 - K^{ij} K_{ij} &= 16\pi\rho \\
\nabla_i \left(K^{ij} - \gamma^{ij} K \right) &= 8\pi S^j
\end{aligned}$$

reduce to a system of five coupled, nonlinear elliptic equations for the lapse function, conformal factor, and the shift vector:

CFC approximation

$$\gamma_{ij} = \phi^4 \delta_{ij}$$

$$\boxed{\begin{aligned}
\hat{\Delta}\phi &= -2\pi\phi^5 \left(\rho h W^2 - P + \frac{K_{ij}K^{ij}}{16\pi} \right) \\
\hat{\Delta}(\alpha\phi) &= 2\pi\alpha\phi^5 \left(\rho h (3W^2 - 2) + 5P + \frac{7K_{ij}K^{ij}}{16\pi} \right) \\
\hat{\Delta}\beta^i &= 16\pi\alpha\phi^4 S^i + 2\phi^{10} K^{ij} \hat{\nabla}_j \left(\frac{\alpha}{\phi^6} \right) - \frac{1}{3} \hat{\nabla}^i \hat{\nabla}_k \beta^k
\end{aligned}}$$

Numerical code

MCoCoA / CoCoNuT code

(Dimmelmeier, Font & Müller 2002, Cerdá-Durán et al 2008)

www.mpa-garching.mpg.de/hydro/COCONUT

- General relativistic ideal MHD code + dynamical spacetime.
- Spherical polar coordinates (2D axisymmetry)
- Godunov-type (HRSC) schemes for the GRMHD solver.
- Spectral methods for the metric solver (elliptic part) LORENE library.

www.lorene.obspm.fr

- Widely tested and applied in the community in studies of relativistic core collapse and evolutions of neutron stars.

Simulations: magneto-rotational core collapse

Understanding gravitational stellar core collapse is one of the primary problems in relativistic astrophysics (since the 1960s)

Distinctive example of a research field where essential progress has been accomplished through numerical modelling with increasing levels of complexity in the input physics/mathematics: hydrodynamics + gravity + magnetic field + Nuclear matter EOS + MHD + transport + ...

Relativistic MHD simulations only possible very recently.

Weakest point of simulations:

Strength and distribution of the initial magnetic field in the core unknown.

If initially weak, several amplification mechanisms may operate: differential rotation Ω-dynamo, MRI.

Status of core collapse simulations

Microphysics	Gravity: Newtonian	Gravity: Modified Newtonian (TOV-like potentials)	Gravity: Approximately relativistic (PPN, CFC, CFC+)	Gravity: Fully relativistic (ADM, ADM-BSSN, MCE)
Ideal gas	✓	✓	✓	✓
Tabulated EoS	✓	✓	ongoing work	ongoing work
Simple neutrino treatment	ongoing work	ongoing work	experimental	experimental
Boltzmann neutrino transport	ongoing work	ongoing work		

(table courtesy of Harry Dimmelmeier)

Relativistic MHD simulations available only very recently

Role of magnetic fields

- **Standard model**: convectively supported neutrino-driven SNe
- **Progenitors**: slowly rotating & weakly magnetized (10^9 - 10^{10} G) (Heger et al 2005)
- **Most ordinary SNe**: Magnetic fields and rotation are not crucial
- **General relativity**: Modified Newtonian potential (TOV) is sufficient for slowly rotating models (Dimmelmeier et al 2006)

- **However**:
  - **Neutron Stars**: strong magnetic field (10^{12} - 10^{13} G)
  - **Magnetars**: 10^{14} - 10^{15} G
  - Subset of **rapidly rotating progenitors** (<1%) (Woosley & Heger 2006)
  - (Long-Soft) **gamma-ray bursts** (collapsar model): Genuine **general relativistic effects** appear (rapid rotation, **black hole formation**)

Initial model

- S20 model of Woosley et al 2002 (iron core of 20 $M_\odot$ star)
- SHEN EOS
- Deleptonization scheme (Liebendörfer 2005), not valid after bounce
- Magnetic field:
  - Poloidal: circular current loop at 400 km
  - $|B_{c0}|=3.54\times10^{10}$ G **(B10)**; $|B_{c0}|=3.54\times10^{12}$ G **(B12)**

$$\vec{B}^* = \hat{\nabla} \times \vec{A}^* \longrightarrow \left.\begin{array}{rcl} B^{*r} &=& \dfrac{1}{r\sin\theta}\dfrac{\partial}{\partial\theta}\left(\sin\theta A^*_\varphi\right) \\ B^{*\theta} &=& -\dfrac{1}{r}\dfrac{\partial}{\partial r}\left(r A^*_\varphi\right) \end{array}\right\}$$

Choose a vector potential such that the associated B-field is divergence-free

B-field generated by a circular current loop

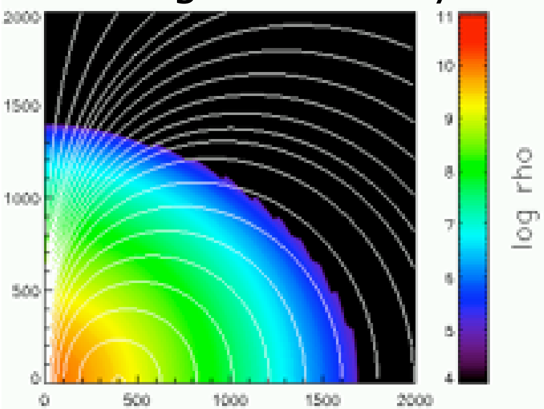

$$A^*_\varphi = \frac{r^2_{\rm mag} B^*_0}{2} \sum_{n=0}^{\infty} \frac{(-1)^n (2n-1)!!}{2^n (n+1)!} \frac{r_<^{2n+1}}{r_>^{2n+2}} P^1_{2n+1}(\cos\theta)$$

$$r_< = \min(r, r_{\rm mag}),\ r_> = \max(r, r_{\rm mag})$$

$$r \ll r_{\rm mag} \longrightarrow \left.\begin{array}{rcl} B^{*r} &\approx& B^*_0 \cos\theta \\ B^{*\theta} &\approx& B^*_0 \sin\theta \end{array}\right\} \qquad r \gg r_{\rm mag} \longrightarrow \left.\begin{array}{rcl} B^{*r} &\approx& 2B^*_0 \dfrac{\cos\theta}{r^3} \\ B^{*\theta} &\approx& B^*_0 \dfrac{\sin\theta}{r^3} \end{array}\right\}$$

Animation of a representative simulation

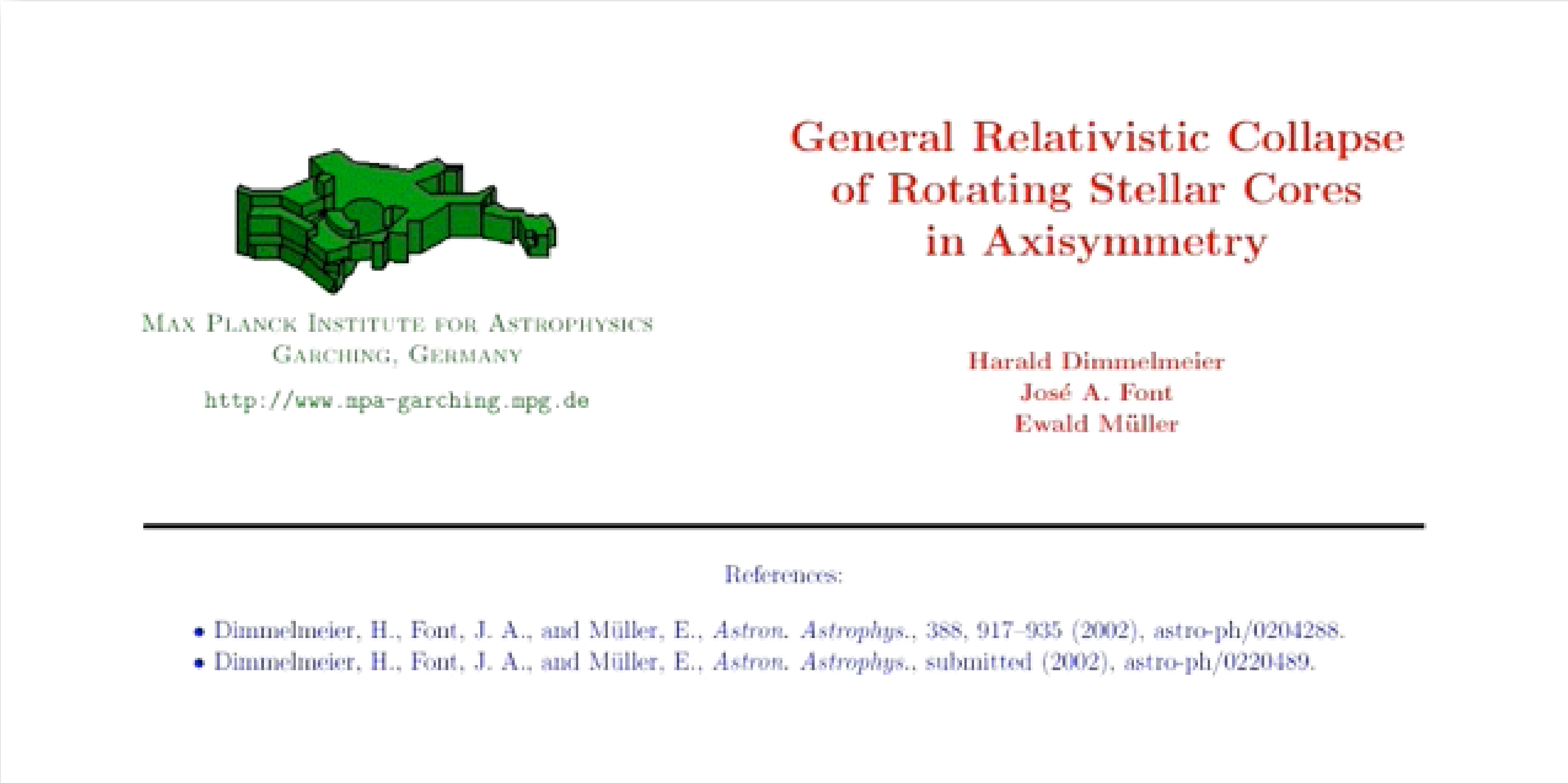

Unmagnetized model (for illustration purposes)

For movies of additional models visit:

www.mpa-garching.mpg.de/rel_hydro/axi_core_collapse/movies.shtml

B10 (weak) vs B12 (strong) time evolutions

Evolution of the central rest-mass density

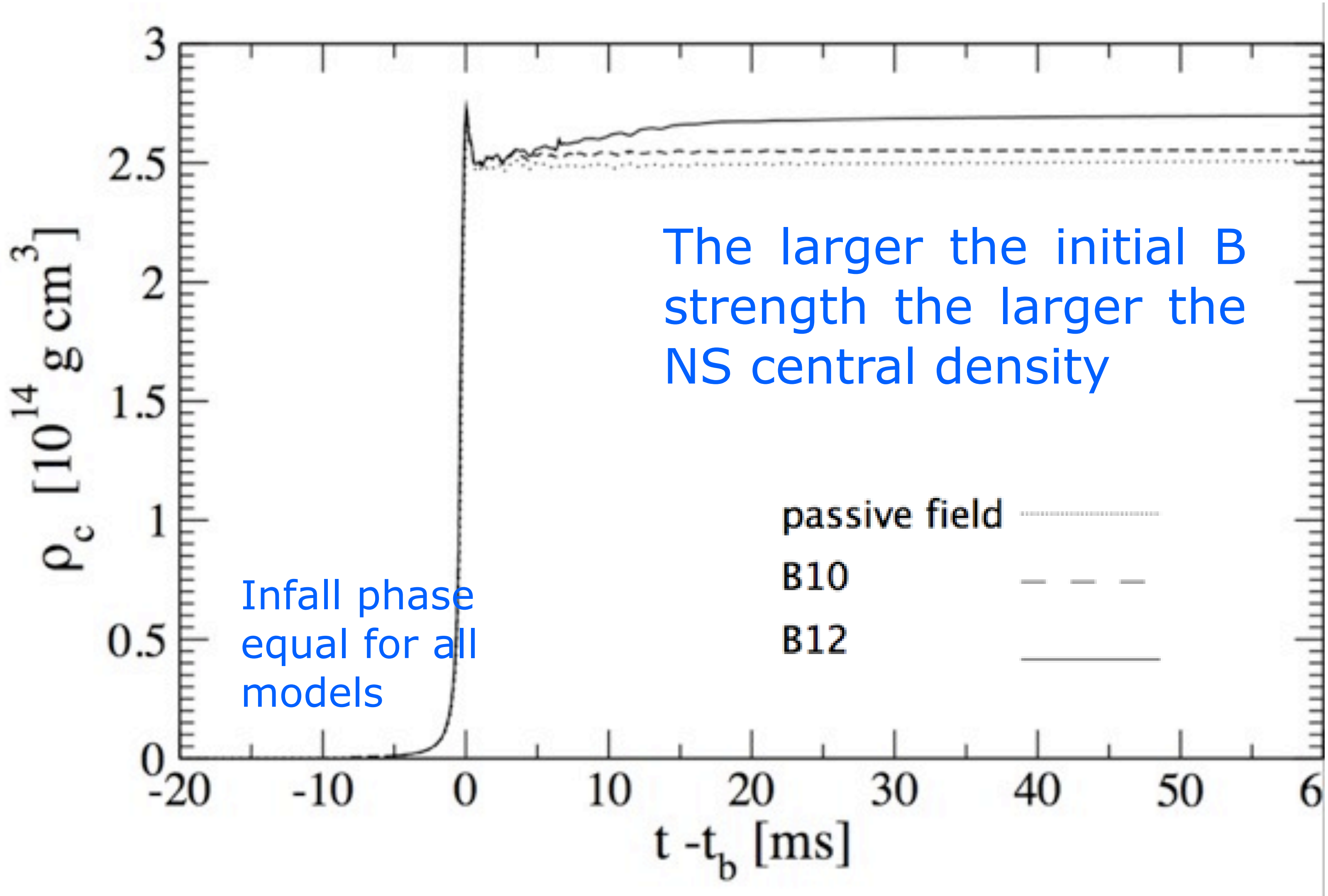

B10 (weak) vs B12 (strong) time evolutions

Evolution of the normalized total magnetic field energy

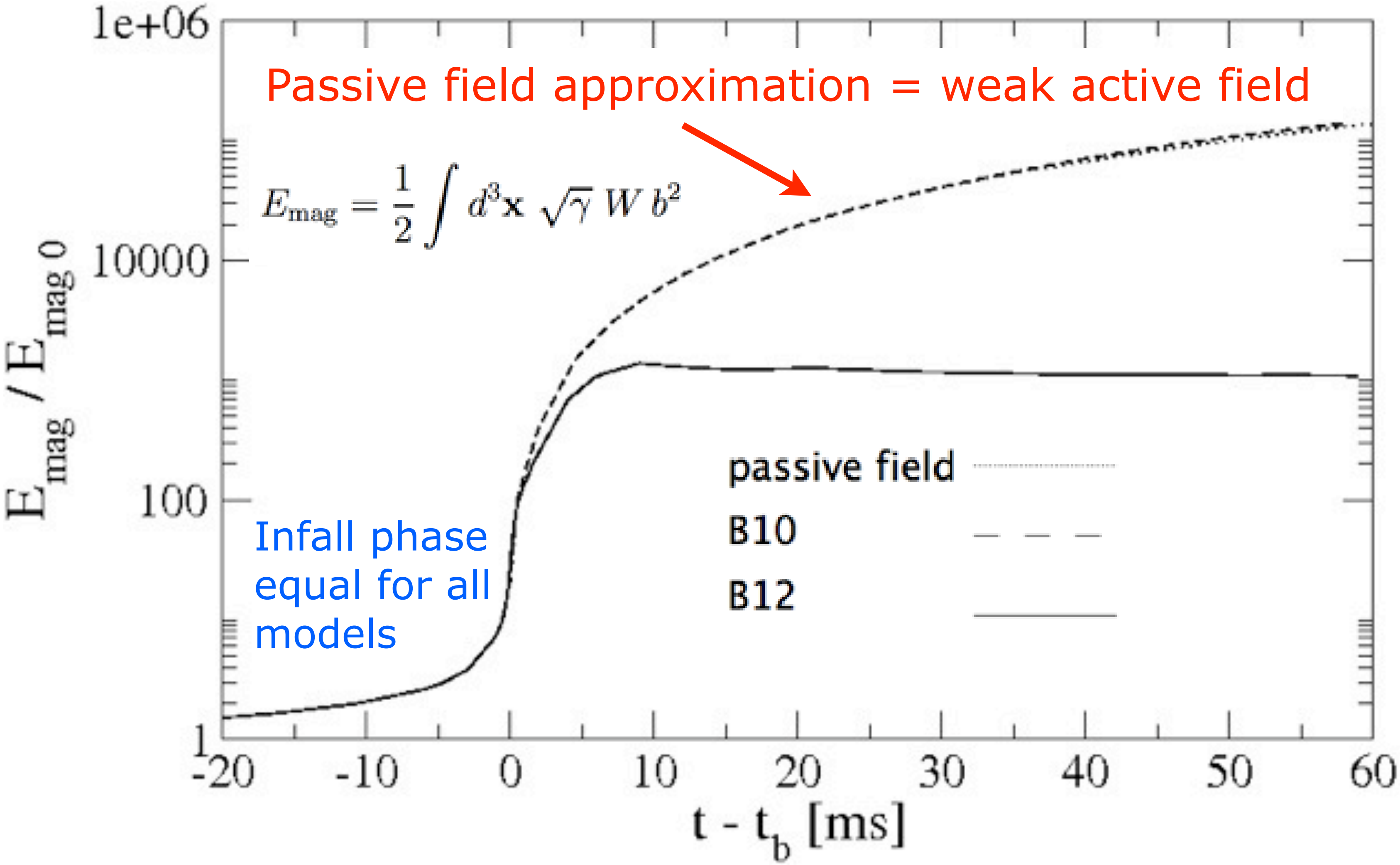

Weak polar outflows

Magnetic field structure (51 ms after core bounce)

Weak field (B10):
similar to the passive
B-field simulations

Strong field (B12):
Polar outflow
- strongly magnetized
- mildly relativistic (W<2)

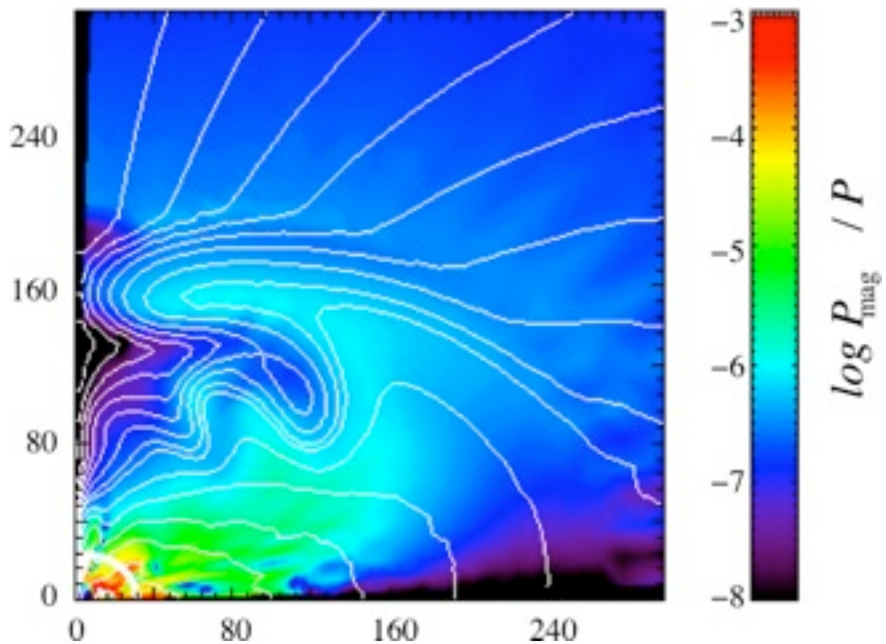

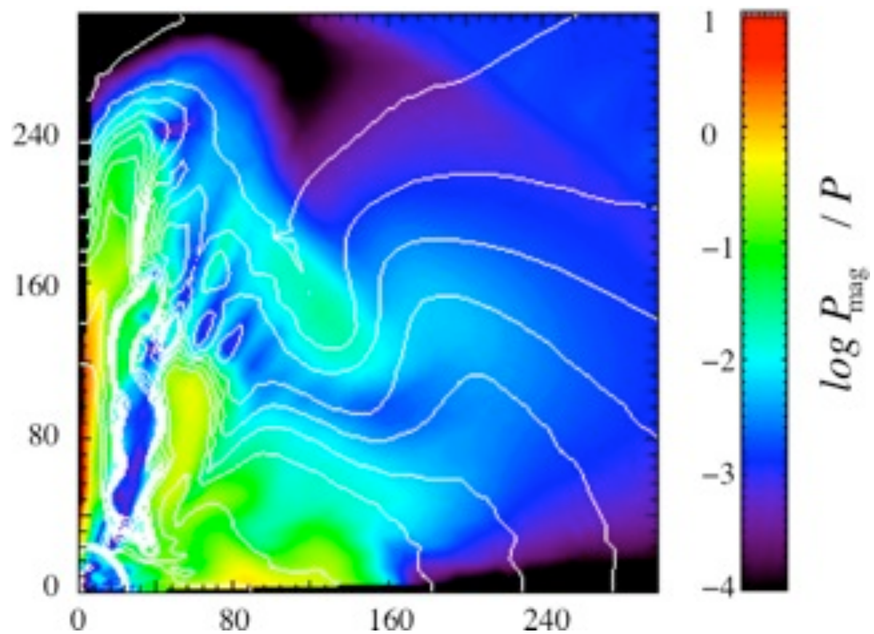

Towards magneto-rotational core collapse

Angular velocity profiles: **B10** (weak field)

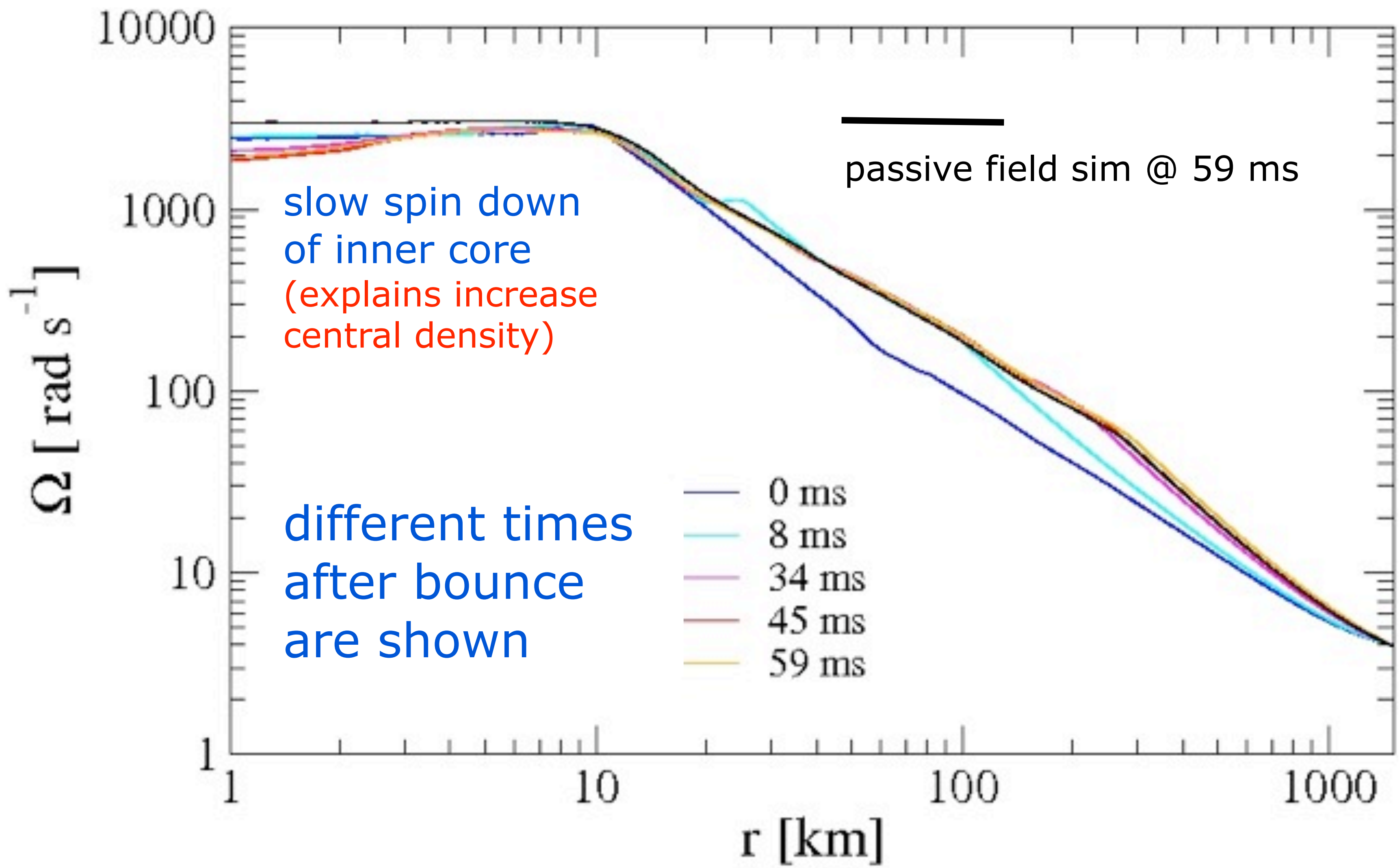

Towards magneto-rotational core collapse

Angular velocity profiles: **B12** (strong field)

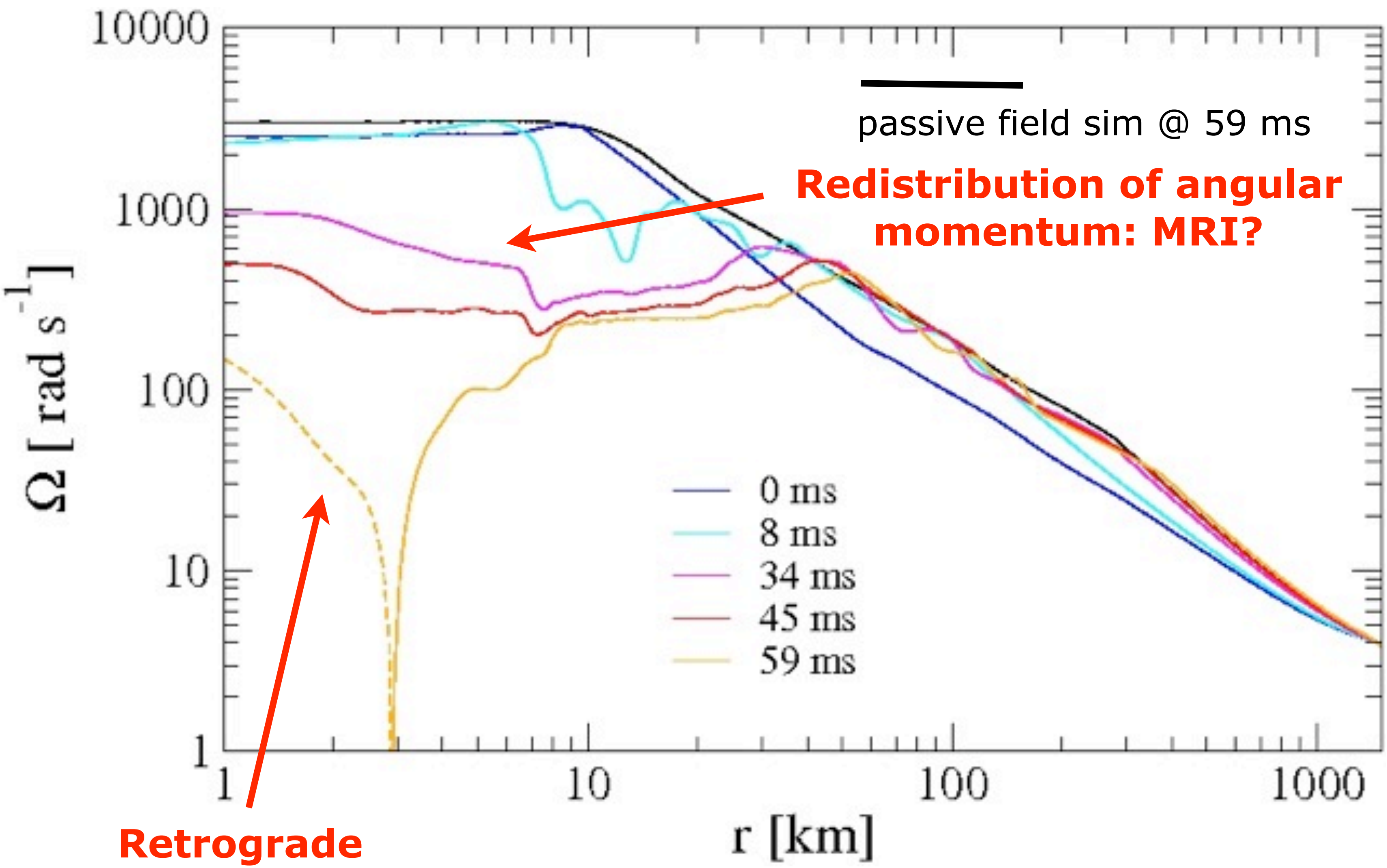

Towards magneto-rotational core collapse

Evolution of the central angular velocity

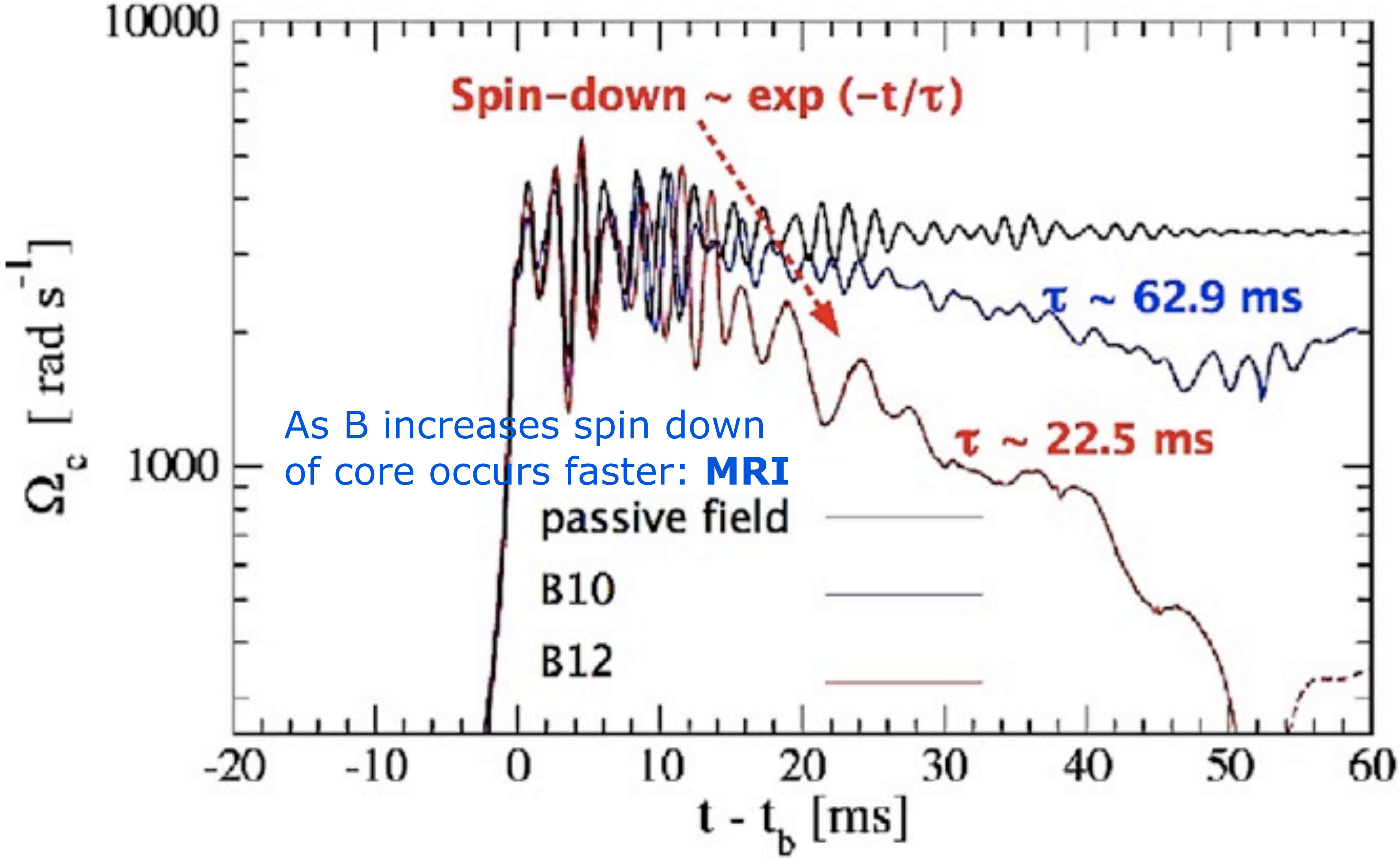

As B increases spin down of core occurs faster: **MRI**

Amplification of the magnetic field (1)

- **Radial compression (RC)**
  (Not very efficient)

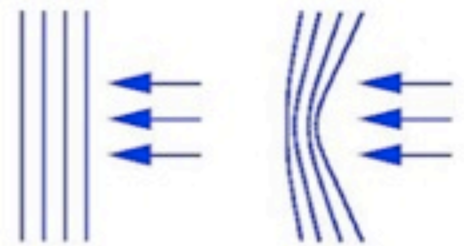

- **Ω-dynamo:** Progenitors with 10^6–10^{10}G ~ **several hours-s**

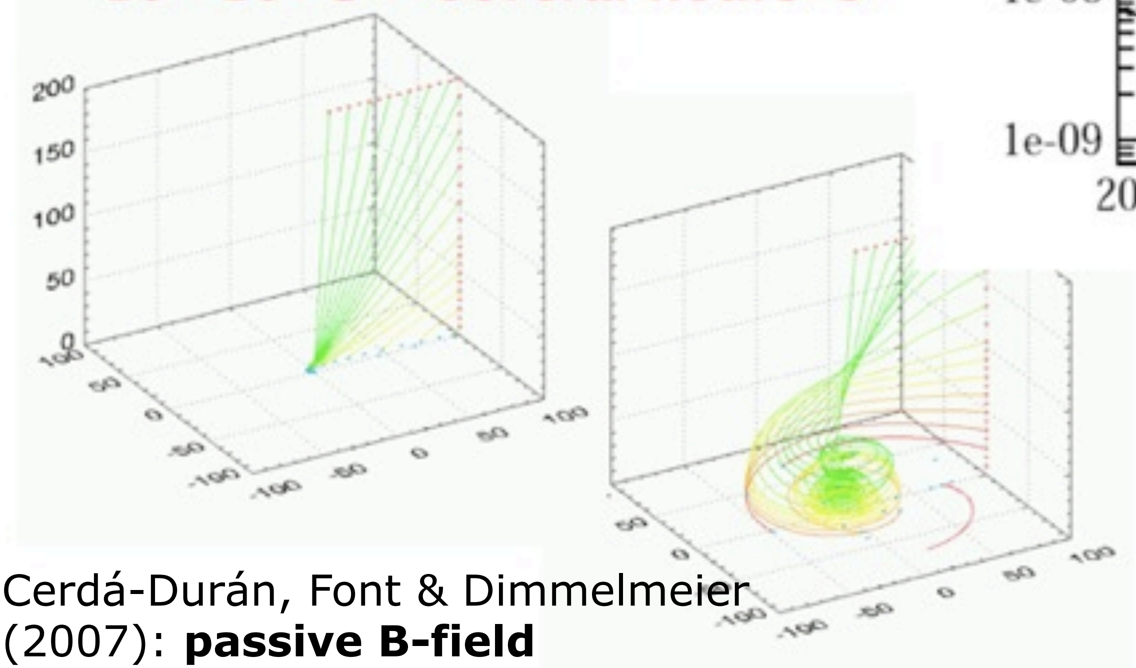

Cerdá-Durán, Font & Dimmelmeier (2007): **passive B-field**

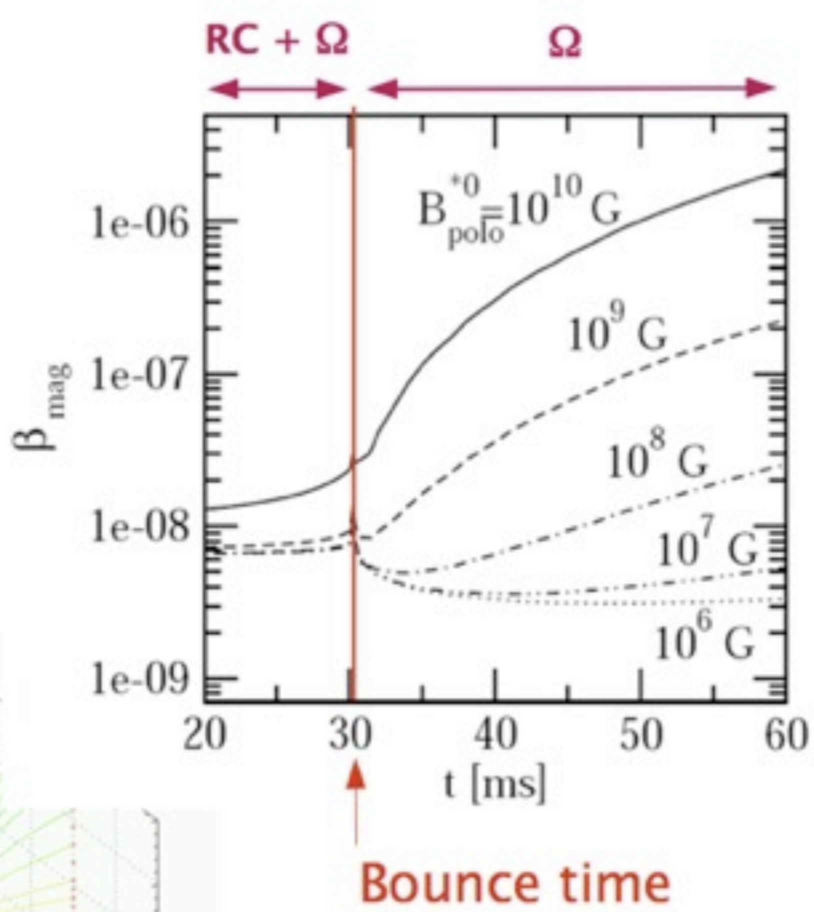

$$B^{*0}_{toroidal} = 10^{10}\ \mathrm{G}$$

$$\boxed{\beta_{mag} = E_{mag} \,/\, |E_{pot}|}$$

Amplification of the magnetic field (2)

Magneto-rotational instability (MRI) (Balbus & Hawley 1991)

MRI is a shear instability that generates turbulence and an amplification of the magnetic field in rotating magnetized plasma, transporting angular momentum in the star (Balbus & Hawley 1991).

Magnetized collapse models are indeed susceptible of developing MRI (Akiyama et al 2003; Obergaulinger et al 2005).

The (Newtonian) condition for the MRI to occur (neglecting buoyancy effects and if the B-field strength is very low) is:

$$\frac{d\Omega^2}{d\ln\varpi} < 0$$

If this condition is fulfilled and the magnetic field has a poloidal component, MRI grows exponentially in time.

The timescale of the fastest growing unstable mode is:

$$\tau_{\rm MRI} = 4\pi \left|\frac{d\Omega}{d\ln\varpi}\right|^{-1}$$

independent of B-field configuration and strength

Towards magneto-rotational core collapse

Magneto-rotational instability (MRI) (Balbus & Hawley 1991)

- MRI unstable: magnetic field + Ω decreases outwards
- Critical length-scale $\sim 2\pi\, C_A / \Omega \sim$ 1-5 km (PNS) for B12
  $\sim$ 10-50m (PNS) for B10
- Time-scale (fastest growing mode) $\sim$ **10 ms** (PNS)

B12: MRI marginally resolved ($\sim$5 points / length-scale)

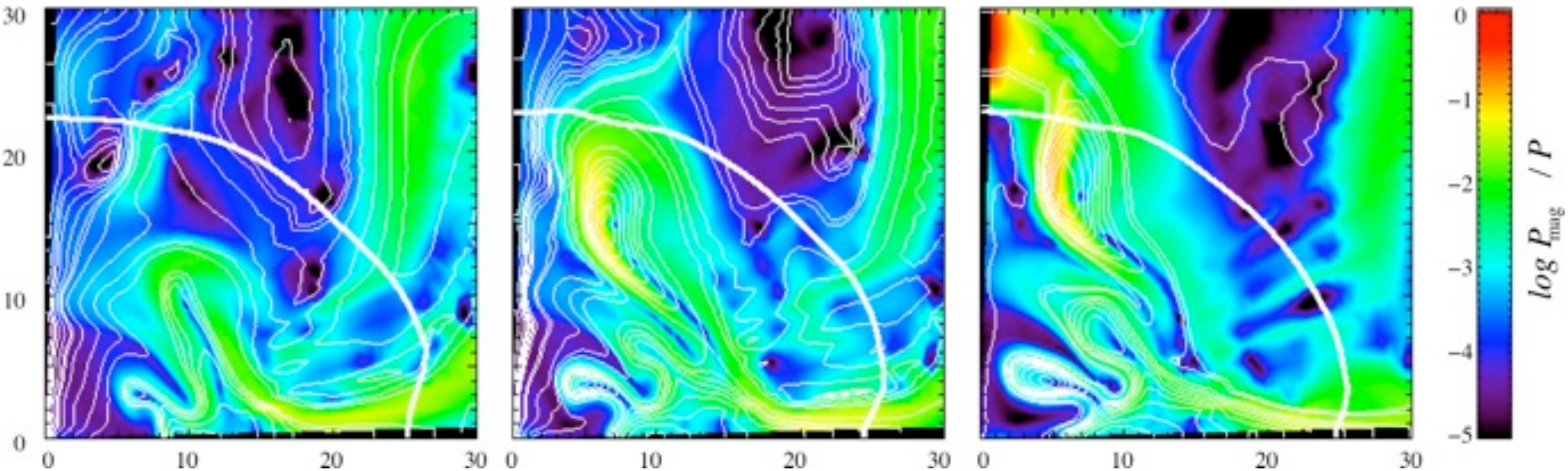

Towards magneto-rotational core collapse

Magneto-rotational instability (MRI) (Balbus & Hawley 1991)

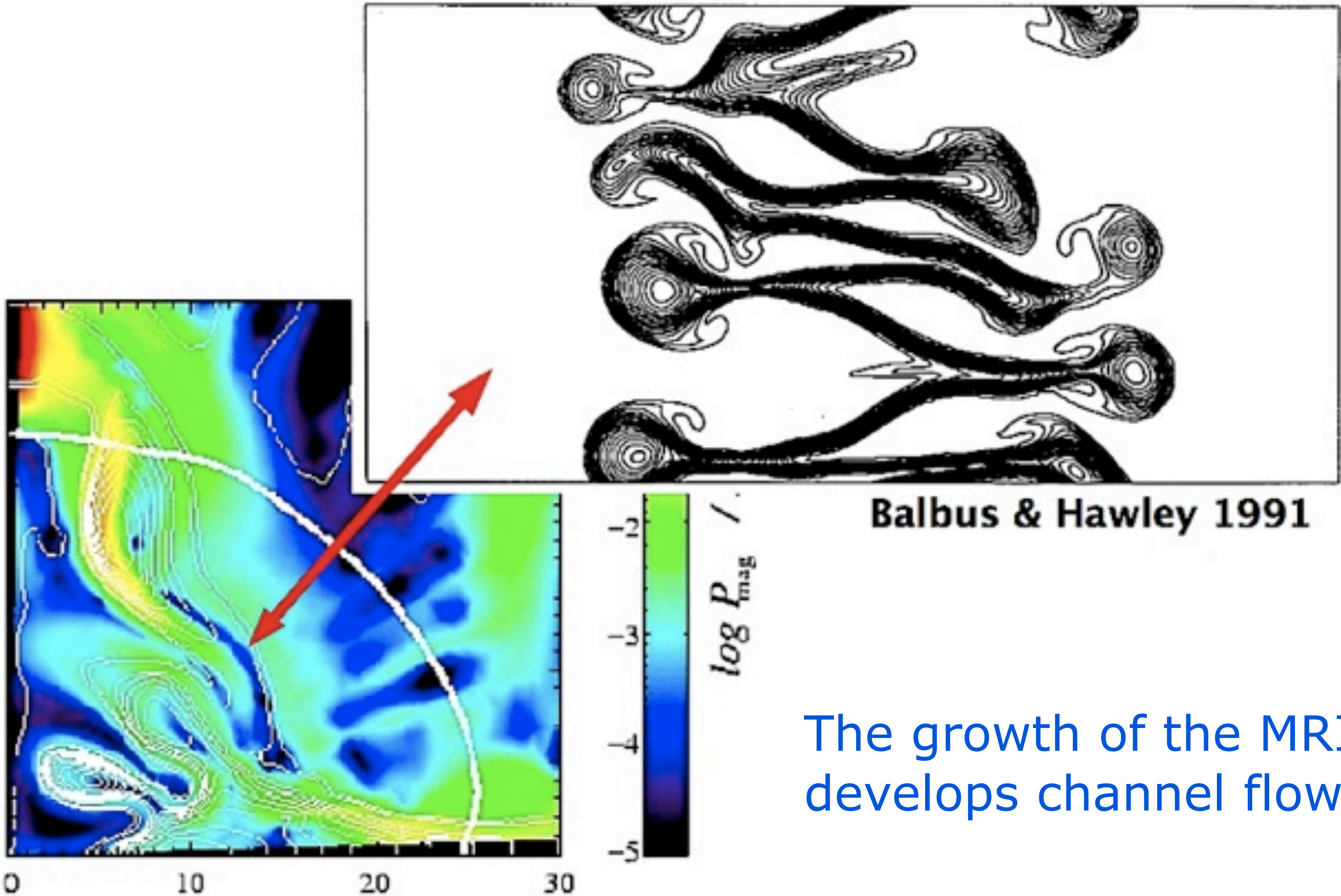

The growth of the MRI develops channel flows.

Magnetars and giant flares in SGRs

Soft gamma repeaters: peaks of gamma-ray flare activity (10^{44}-10^{46} erg/s in ~0.2 s) followed by a decaying X-ray tail (~100 s)

SGRs are a class of magnetars (Duncan & Thomson 1992): neutron stars with very strong magnetic fields ($B>10^{14}$G)

Three giant flares have been detected so far:

- SGR 0526-66 on March 5, 1979
- SGR 1900+14 on August 27, 1998
- SGR 1806-20 on December 27, 2004

Magnetar bursts are magnetic-field-driven quakes in the crust of neutron stars.

QPOs in the decaying X-ray tail

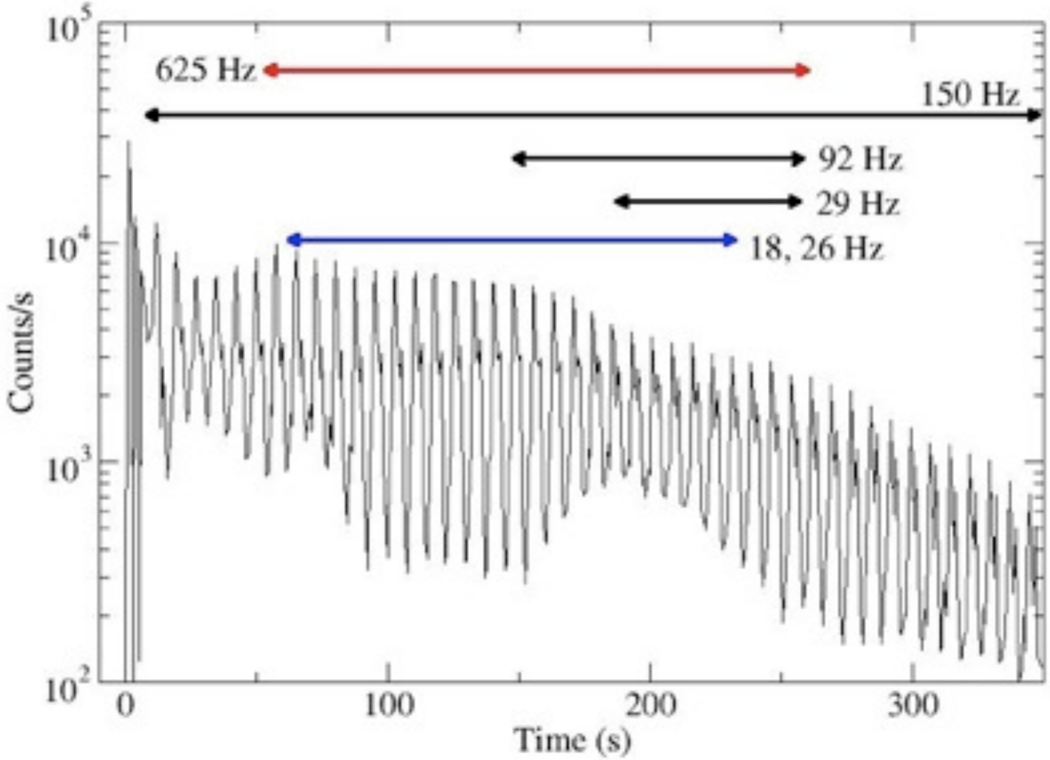

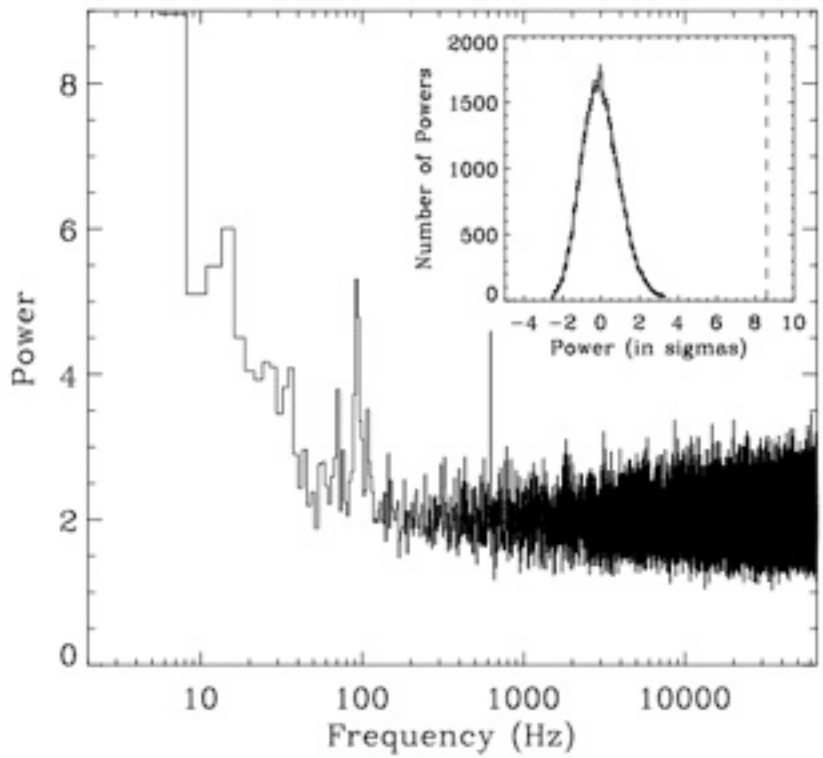

High frequency variations (QPOs) discovered in the tail of the 2004 flare from SGR 1806-20 using data from RXTE and RHESSI (Israel et al. 05, Watts & Strohmayer 06, Strohmayer & Watts 06).

Similar QPOs discovered in the tail of the 1998 flare from SGR 1900+14 using RXTE data (Strohmayer & Watts 05).

Model 1: torsional modes of solid crust

(Schumaker & Thorne 1983; Piro 2005; Samuelsson & Andersson 2007)

The QPO frequencies are in broad good agreement with models of torsional shear modes of neutron star crusts. Fails to explain all (low ~20Hz) frequencies.

Model 2: Alfvén QPO model

(Glampedakis et al 2006; Levin 2006; Levin 2007; Sotani et al 2007, 2008; Colaiuda et al 2009, Cerdá-Durán et al 2009)

Both, global (crust-core coupling) elasto-magnetic oscillations and pure Alfvén oscillations.

- Continuum of Alfvén oscillations
- QPOs at turning points and edges

Here: **first GRMHD simulations**

Cerdá-Durán, Stergioulas & Font, MNRAS, **397**, 1607 (2009)
Gabler, Cerdá-Durán, Font, Stergioulas & Müller, in preparation

Nonlinear evolutions (hydrodynamics + spacetime): promising new approach introduced in recent years for computing mode frequencies (Font et al 2000, 2001, 2002; Stergioulas et al 2001, 2004; Dimmelmeier et al 2005).

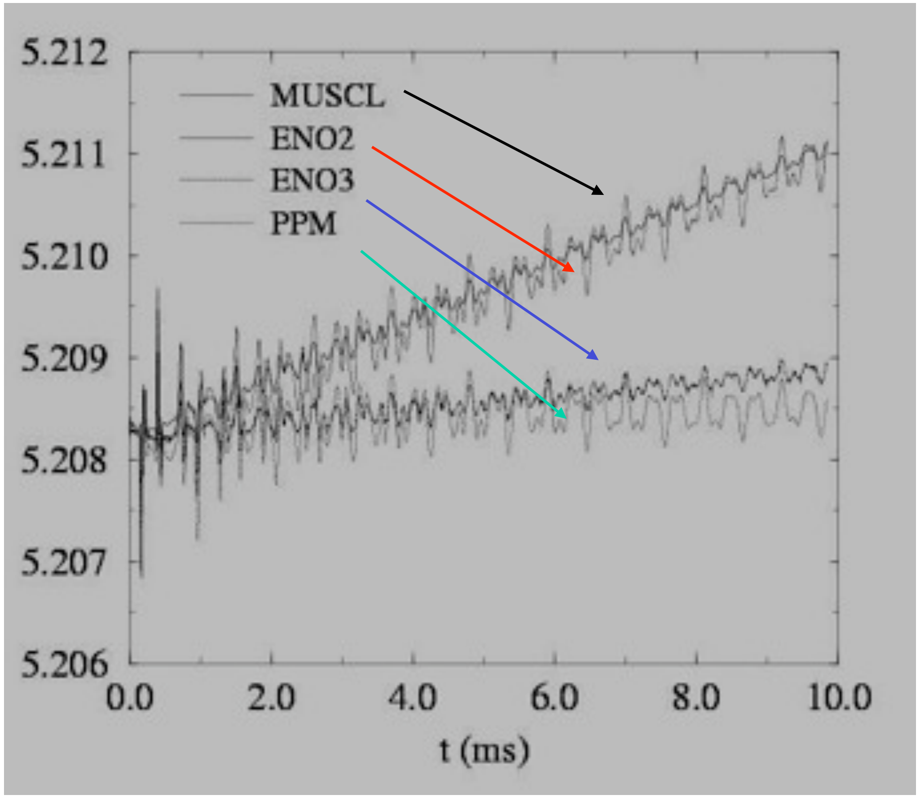

The higher the order the smaller the drift

Font, Stergioulas, Kokkotas (2000)

Simulations show the appearance of linear **pulsation modes**, harmonics (overtones) and nonlinear harmonics.

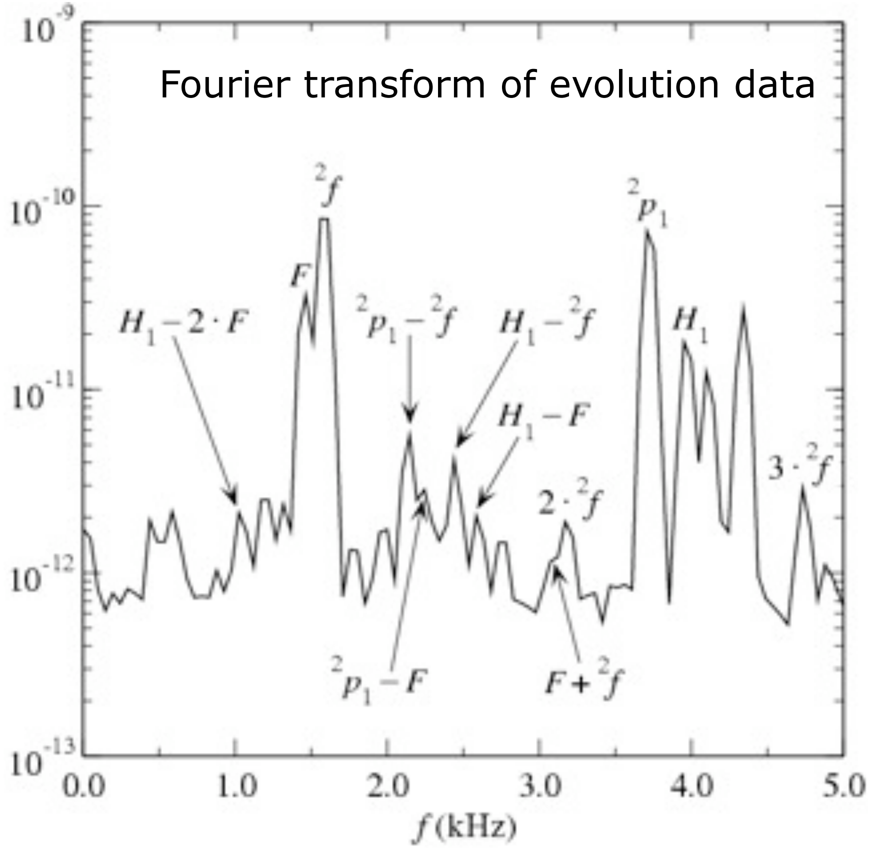

Dimmelmeier, Stergioulas, Font (2006)

Magnetar models and main simplifications

Model	R_e [km]	r_e [km]	$r_p/r_e - 1$	M [$M_\odot$]	$B_{\rm polar}$ [G]	ρ_c[g cm^{-3}]	j_0 [A m^{-2}]	current function
MNS1	14.155	11.998	8×10^{-6}	1.40	6.5×10^{14}	7.91×10^{14}	2×10^{13}	Bocquet et al. (1995)
MNS2	14.157	11.999	8×10^{-4}	1.40	6.5×10^{15}	7.91×10^{14}	2×10^{14}	Bocquet et al. (1995)
MNS3	14.168	12.006	5×10^{-3}	1.40	1.6×10^{16}	7.91×10^{14}	5×10^{14}	Bocquet et al. (1995)
LMNS2	15.153	13.322	10^{-3}	1.20	5.1×10^{15}	5.47×10^{14}	2×10^{14}	Bocquet et al. (1995)
HMNS2	12.444	9.941	4×10^{-4}	1.60	8.4×10^{15}	1.37×10^{15}	2×10^{14}	Bocquet et al. (1995)
S1	14.153	11.912	0	1.40	4.0×10^{15}	7.91×10^{14}	N/A	Sotani et al. (2007a)

- Cowling approximation (fixed spacetime metric)
- Small-amplitude torsional perturbations
- Relativistic anelastic approximation (Bonazzola et al 2007)

→ sound waves neglected (long-term evolutions)

$$Y(t=0) = 0 \quad \dot{Y}(t=0) = \alpha v^\varphi = f(r)\, b(\theta)$$

$$f(r) = \sin\left(\frac{3\pi}{2}\frac{r}{R}\right)$$

$$b(\theta) = b_2 \frac{1}{3}\partial_\theta P_2(\cos\theta) + b_3 \frac{1}{6}\partial_\theta P_3(\cos\theta)$$

Only left with evolution equations for S_φ and B^φ

$b_2=0$ ($b_3=0$) symm. (antisymm.) perturbation across equator

Simulations: spatial pattern of effective amplitude

$$\mathcal{A}(r,\theta;f) = \mathrm{FT}\,[\dot{Y}(r,\theta;t)]$$

Amplitude only appreciable along magnetic axis

Non-zero (maximum) amplitude at the surface

Upper QPOs

Number of nodes along magnetic axis and location agrees with nodes computed with semi-analytic model

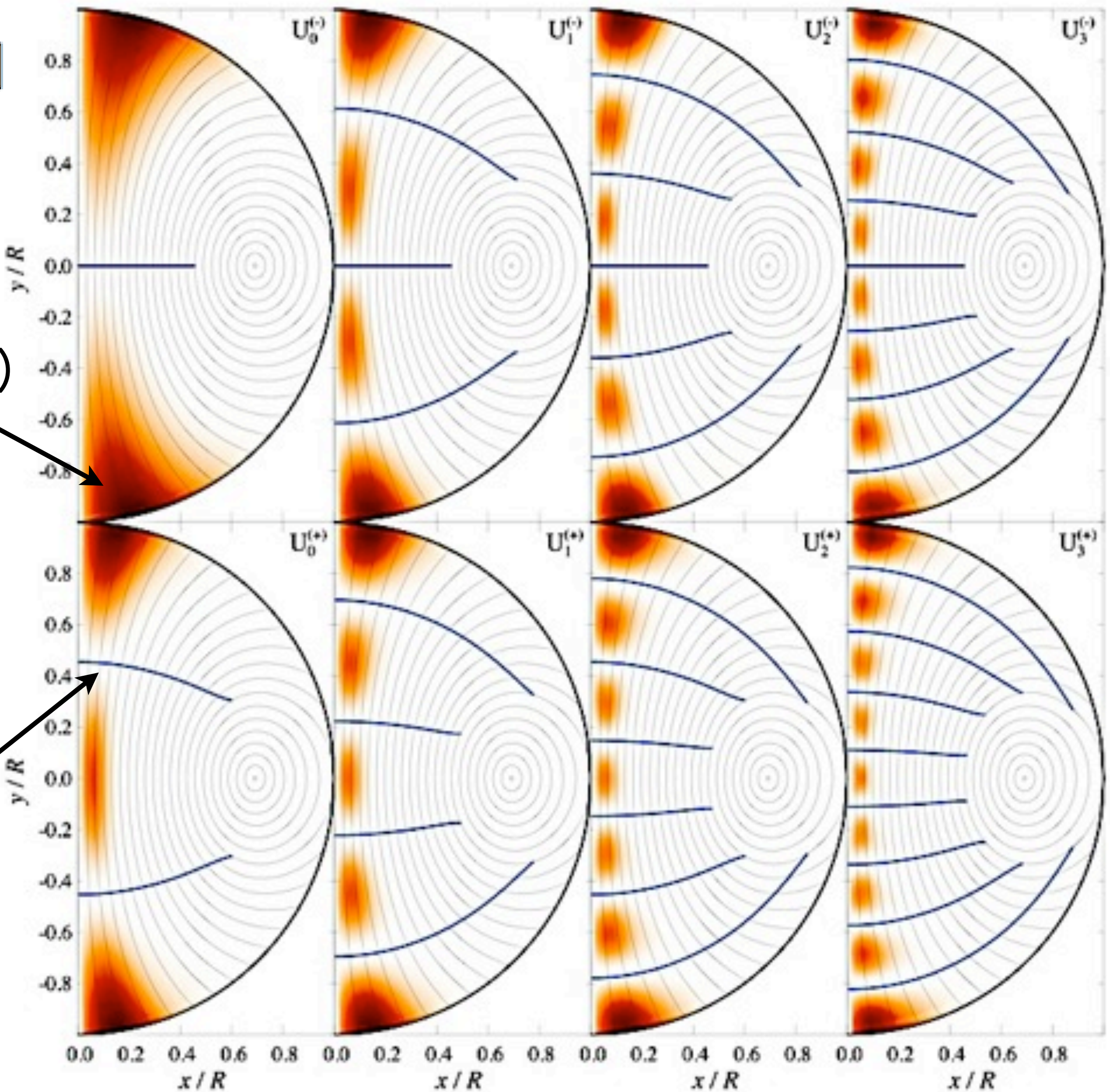

Simulations: spatial pattern of effective amplitude

Lower QPOs

Amplitude only appreciable within the region of closed field lines

QPO at the turning point

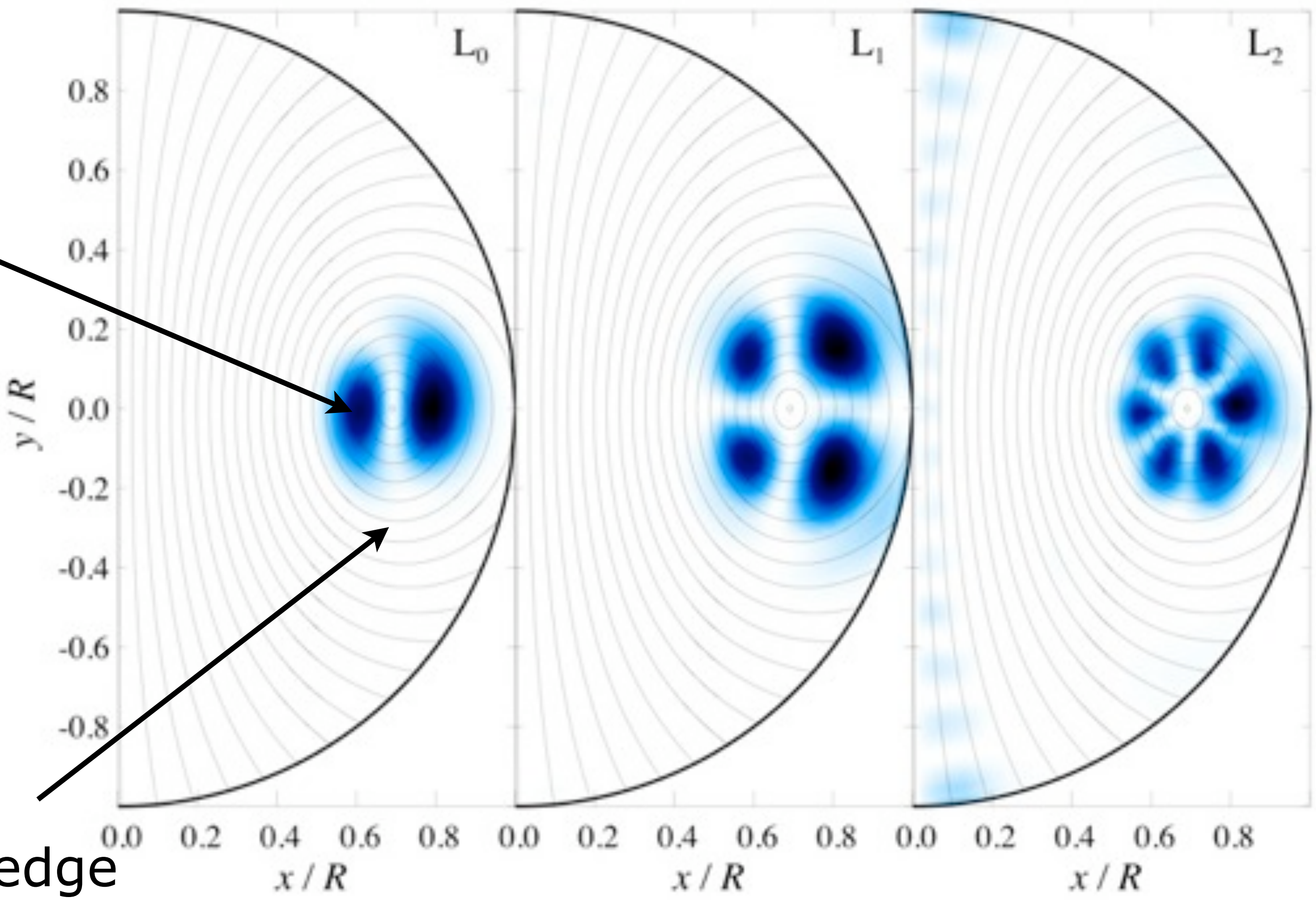

No QPO at the edge

(but Colaiuda et al 2009 find QPOs at the edge)

Inclusion of a solid crust (Gabler's talk)

$$T^{\mu\nu} = \rho h^* u^\mu u^\nu + p^* g^{\mu\nu} - b^\mu b^\nu \boxed{- 2\mu_{\rm shear}\Sigma^{\mu\nu}}$$

$$\frac{1}{\sqrt{-g}}\left(\frac{\partial\sqrt{\gamma}\mathbf{U}}{\partial x^0} + \frac{\partial\sqrt{-g}\mathbf{F}^i}{\partial x^i}\right) = 0$$

$$\mathbf{U} = (S_\varphi, B^\varphi) \qquad \Sigma^{i\varphi} = \frac{1}{2}g^{ii}\xi^\varphi{}_{,i}$$

$$\mathbf{F}^i = \left(-\frac{b_\varphi B^i}{W}\boxed{- 2\mu_{\rm shear}\Sigma^i{}_\varphi}, -v^\varphi B^i\right) \qquad (i = r, \theta)$$

$$(\xi^\varphi{}_{,i})_{,t} - (\alpha v^\varphi)_{,i} = 0 \qquad (i = r, \theta)$$

Test: limiting cases of zero shear (Cerdá-Durán et al 2009) and zero magnetic field (Sotani et al 2007) are recovered.

Damping of crustal shear modes

Model: APR+DH EOS, $M=1.4M_{sun}$, R=12.26km, Dipolar magnetic field

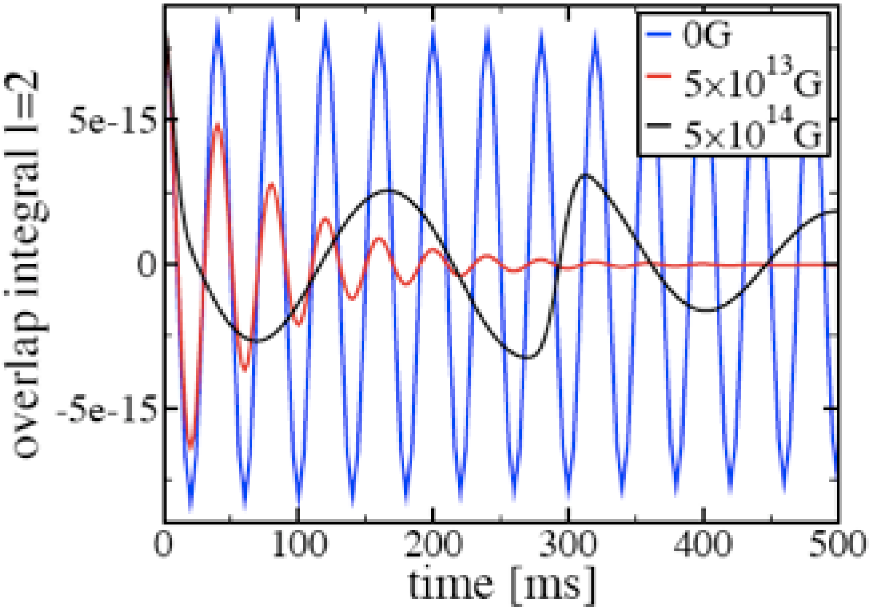

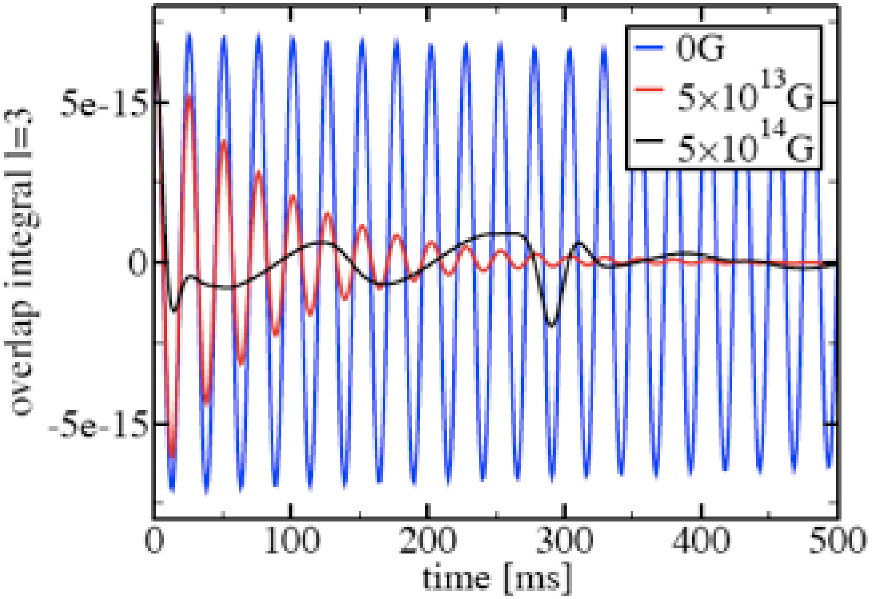

- Strong damping of n=0 crustal modes on a timescale of ~100ms for $5\text{x}10^{13}$G fields.

- After the damping of crustal models only remain coupled magneto-ellastic oscillations.

Alfvén QPOs in the core

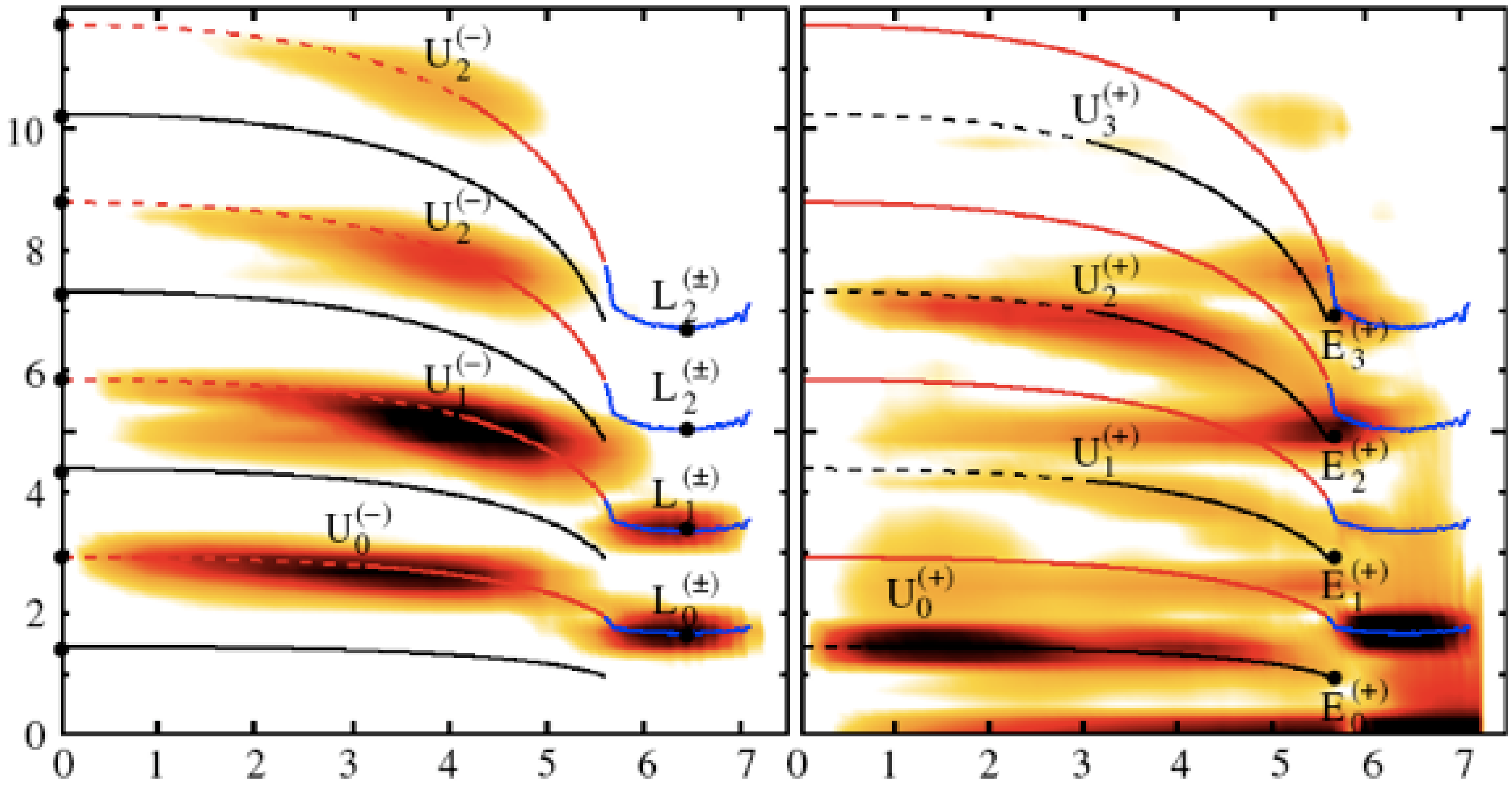

- Lower (turning point) QPOs at closed field lines (as in the zero crust case since closed lines unaffected by crust).
- Upper QPOs in the continuum but further away from the pole than in the zero crust model.
- Edge QPOs at the edges of the continuum.

Summary

- MHD simulations of magneto-rotational core collapse in general relativity feasible nowadays.
  - Strongly magnetized, mildly relativistic polar outflows.
  - Amplification of the B-field by MRI.

- Study of Alfvén/shear oscillations in magnetars using nonlinear MHD simulations (anelastic approximation).
  - Alfvén oscillations form a continuum in the core of magnetars.
  - Lower, Edge, and Upper QPOs.
  - Strong damping of crustal modes for magnetic field strengths well below magnetar levels. No longer valid interpretation for the observed long-lived QPOs in SGR giant flares.